Translational Stroke Research (2019) 10:112–119
https://doi.org/10.1007/s12975-018-0669-0

ORIGINAL ARTICLE

Brain Ceruloplasmin Expression After Experimental Intracerebral Hemorrhage and Protection Against Iron-Induced Brain Injury

Hongwei Liu[1,2] · Ya Hua[1] · Richard F. Keep[1] · Guohua Xi[1]

Received: 16 July 2018 / Revised: 1 October 2018 / Accepted: 2 October 2018 / Published online: 12 October 2018

Abstract

Ceruloplasmin (CP) is an essential ferroxidase that is involved in maintaining iron homeostasis by oxidizing toxic ferrous iron (Fe^{2+}) to less-toxic ferric iron (Fe^{3+}). CP has been well studied in many neurodegenerative diseases, but there has not been an in-depth investigation in intracerebral hemorrhage (ICH). This research investigated brain CP expression in rats after ICH and the effect of CP on Fe^{2+}-induced brain injury. This study had two parts: first, rats had injection of autologous blood into the right basal ganglia and the time course of CP expression in the brain examined (protein and mRNA). Second, rats had an injection of either Fe^{2+} in saline, Fe^{2+} plus CP in saline, or saline alone into the right basal ganglia. All rats in the second part had T2-weighted magnetic resonance imaging, and behavioral tests before the brains were harvested for immunohistochemistry and Western blotting. We found that CP was expressed on neurons and astrocytes in both cortex and basal ganglia after ICH. The time course showed that ICH induced CP expression increased from 4 h to 7 days, peaking at day 3. Whether the brain itself can produce CP was confirmed by RT-PCR. Exogenous CP reduced Fe^{2+}-induced T2 lesions, blood-brain barrier disruption, brain cell death, and neurological deficits. These results suggest a role of CP in potentially reducing ICH-induced brain injury.

Keywords Blood-brain barrier disruption · Cerebral hemorrhage · Ceruloplasmin · Iron · Neuronal death

Introduction

Brain iron accumulation has a critical role in brain damage following intracerebral hemorrhage (ICH) [1, 2]. Iron overload after ICH leads to oxidative stress, blood-brain barrier leakage, brain edema, and brain cell death [1, 3, 4].

Ceruloplasmin (CP) is an abundant plasma glycoprotein that has ferroxidase activity. It can oxidize ferrous iron (Fe^{2+}) to less toxic ferric iron (Fe^{3+}) [5]. CP plays a role in brain iron homeostasis [5]. Previous studies have shown that CP is expressed in the cerebral cortex, basal ganglia, hippocampus, and cerebellum in the central nervous system [6]. Accumulated evidence demonstrates that CP deficiency is associated with several neurodegenerative diseases such as Alzheimer's disease, Parkinson's disease, and aceruloplasminemia [7]. However, little is known about the role of CP in brain injury after ICH.

The current study examined brain CP expression in a rat model of ICH. The effect of exogenous CP on brain injury induced by ferrous iron was also examined.

Material and Methods

Animal Preparation and Intracerebral Infusion

The University of Michigan Institutional Animal Care and Use Committee approved all animal procedure protocols. A total of 78 adult male Sprague–Dawley (SD) rats (250 to 350 g, Charles River Laboratories, Portage, MI) were used in this study. Four rats died during surgery. Rats were anesthetized with pentobarbital (45 mg/kg; i.p.) and body temperature maintained at 37 °C with a feedback-controlled heating pad. Rats were then placed in a stereotactic frame (David Kopf Instruments, Tujunga, CA) and a cranial burr hole (1 mm) drilled on the right coronal suture 3.5 mm lateral to the midline. A 26-gauge needle was inserted stereotaxically into the right basal ganglia (coordinates: 0.2 mm anterior, 5.5 mm

✉ Guohua Xi
guohuaxi@umich.edu

[1] Department of Neurosurgery, R5018 BSRB, University of Michigan, 109 Zina Pitcher Place, Ann Arbor, MI 48109-2200, USA

[2] Department of Neurosurgery, Xiangya Hospital, Central South University, Changsha, China

ventral, and 3.5 mm lateral to the bregma). Autologous whole blood, ferrous iron, ferrous iron plus ceruloplasmin or saline were injected into the right basal ganglia with a microinfusion pump (Harvard Apparatus Inc.) at a rate of 10 μL/min. Sham controls had only an intracerebral needle insertion. The needle was then removed, the burr hole sealed with bone wax, and the incision sutured.

Experimental Groups

This study included two parts. The rats were randomized by using selection of odd or even numbers. In part one, rats had either needle insertion or intracerebral injection of 100 μL autologous whole blood into the right basal ganglia. The ICH rats were euthanized at 4 h, days 1, 3, and 7 ($n = 9$ each group). Sham rats were euthanized at day 3 ($n = 9$). The brains were processed for histology and RT-PCR.

In part two, rats received a 50 μL intracerebral injection of either 0.2 mM ferrous chloride in saline (Sigma, $n = 10$), 0.2 mM ferrous chloride plus 10 μM ceruloplasmin (LSBio, 25.6 kDa, LS-G13090) in saline ($n = 10$), or saline alone ($n = 9$) into the basal ganglia. All rats had T2-weighted MRI and behavioral tests at 24 h after injection. They were then euthanized and the brains harvested for histological and Western blots.

MRI and T2 Lesion Measurement

Rats were anesthetized with 2% isoflurane/air mixture during MRI examination on a 9.4-T Varian MR scanner (Varian Inc., Palo Alto, CA). A T2 fast spin-echo sequence (TR/TE = 4000/60 ms) using a field of view of 35 × 35 mm^2, matrix of 256 × 256 pixel, and 25 coronal slices (0.5 mm thick) was employed. All MRI images were measured using NIH ImageJ. The T2 lesion was outlined along the border of the hyperintense signal area in the basal ganglia. Total T2 lesion volume was obtained by combining slice thickness (0.5 mm) and multiplying by total areas [8].

Immunohistochemistry and Immunofluorescence Staining

Immunohistochemistry and immunofluorescence staining were performed as previously described [9, 10]. For immunohistochemistry staining, the primary antibodies were rabbit anti-ceruloplasmin IgG (Abcam, ab110449, 1:500), rabbit anti-DARPP-32 IgG (Cell Signaling, 2306S, 1:500), sheep anti-albumin IgG (Bethyl, A110–134, 1:4000), and rabbit anti-cleaved caspase-3 IgG (Cell Signaling, 9661S, 1:400). Negative controls omitted the primary antibody.

For immunofluorescence triple labeling, the primary antibodies were rabbit anti-ceruloplasmin IgG (Abcam, ab110449, 1:200), rabbit anti-NeuN IgG (Abcam, ab104225, 1:500), goat anti-GFAP IgG (Abcam, ab53554, 1:500), and goat anti-Iba-1 IgG (Abcam, ab107159, 1:500) Secondary antibodies were Alexa Fluor 488 donkey anti-rabbit IgG (Invitrogen, 1:500), Fluro 594 donkey anti rabbit IgG (Invitrogen, 1:500), and Fluor 594 donkey anti goat IgG (Invitrogen, 1:500). Nuclei were labeled with DAPI (Sigma-Aldrich, F6057).

Reverse Transcription-Polymerase Chain Reaction (RT-PCR)

RT-PCR analyses were done as described previously [11]. To test the mRNA expression of ceruloplasmin in the brain, total RNA was extracted from the ipsilateral basal ganglia using RNeasy Mini Kit (Qiagen Inc., Valencia, CA). Reverse transcription was performed using the SuperScript First-Strand Synthesis Kit (Invitrogen, Carlsbad, CA). For semiquantitative PCR, 1 μL of target cDNA conversion mixture was amplified using Hotstar Taq DNA Polymerase (Qiagen) for 37 cycles at 94 °C for 20 s, at 53 °C for 25 s, and at 72 °C for 30 s. The PCR primers (NIH GenBank database) included ceruloplasmin (forward, 5′-TGCTTCTGGCAGTGAAGAAA-3′; reverse, 5′-AGGGCCTAGAGGCAAAGTTC-3′; 245 bp), GAPDH (forward, 5′- AAGATGGTGAAGGTCGGTGT-3′; reverse, 5′- GATCTCGCTCCTGGAAGATG -3′; 241 bp). PCR products were visualized by electrophoresis in agarose (1%) gels and stained with SYBR gel stain (Invitrogen). Photographs were taken with Gel Doc XR system (Bio-Rad, Hercules, CA). mRNA expression values were normalized to GAPDH and analyzed using NIH Image J.

Western Blot Analysis

Western blot analysis was performed as described previously [12, 13]. Ipsilateral basal ganglia tissues were sampled. Briefly, protein concentration was measured by Bio-Rad protein assay kit (Hercules, CA), and 50 μg protein of each sample was suspended in loading buffer, denatured at 95 °C for 5 min, and then separated by SDS-PAGE gel and transferred onto a hybond-C pure nitrocellulose membrane (Amersham, PA). Membranes were probed with the primary antibodies after 1 h blocking with nonfat milk buffer. The primary antibodies were sheep anti-albumin IgG (Bethyl laboratories, 1:10000), rabbit anti-DARPP-32 IgG (Cell Signaling Technology, 1:10000), and mouse anti-β actin (Sigma-Aldrich, 1:100000). The secondary antibodies were rabbit anti-sheep IgG (Bio-Rad, 1:2500), goat anti-rabbit IgG (Bio-Rad, 1:2500), and goat anti-mouse IgG (Bio-Rad, 1:5000). Protein band densities were detected by Kodak X-OMAT film. The relative protein densities of bands were performed with NIH ImageJ.

Terminal Deoxynucleotidyl Transferase (TdT) -Mediated dUTP Nick-End Labeling (TUNEL) Assay

According to the instruction of the TUNEL detection kit (S7100, Temecula, CA), double-strand DNA damage was detected by TUNEL staining.

Cell Counting

The number of positive cells was counted in three different areas of each brain coronal section. Using a digital camera to take three high-power images (× 40 magnification) in the cortex or basal ganglia. A blinded observer performed all counting which was repeated three times and the mean value calculated.

Behavioral Tests

Corner-turn and forelimb-use asymmetry tests were used for behavioral assessment as previously described [14]. The two behavioral tests were evaluated by an investigator blinded to treatment.

Statistical Analysis

All values are expressed as mean ± SD. Data were analyzed with Student's *t* test, one-way ANOVA test with Tukey post hoc test or two-way ANONA with Sidak's post hoc test. Significant levels were set at $P < 0.05$.

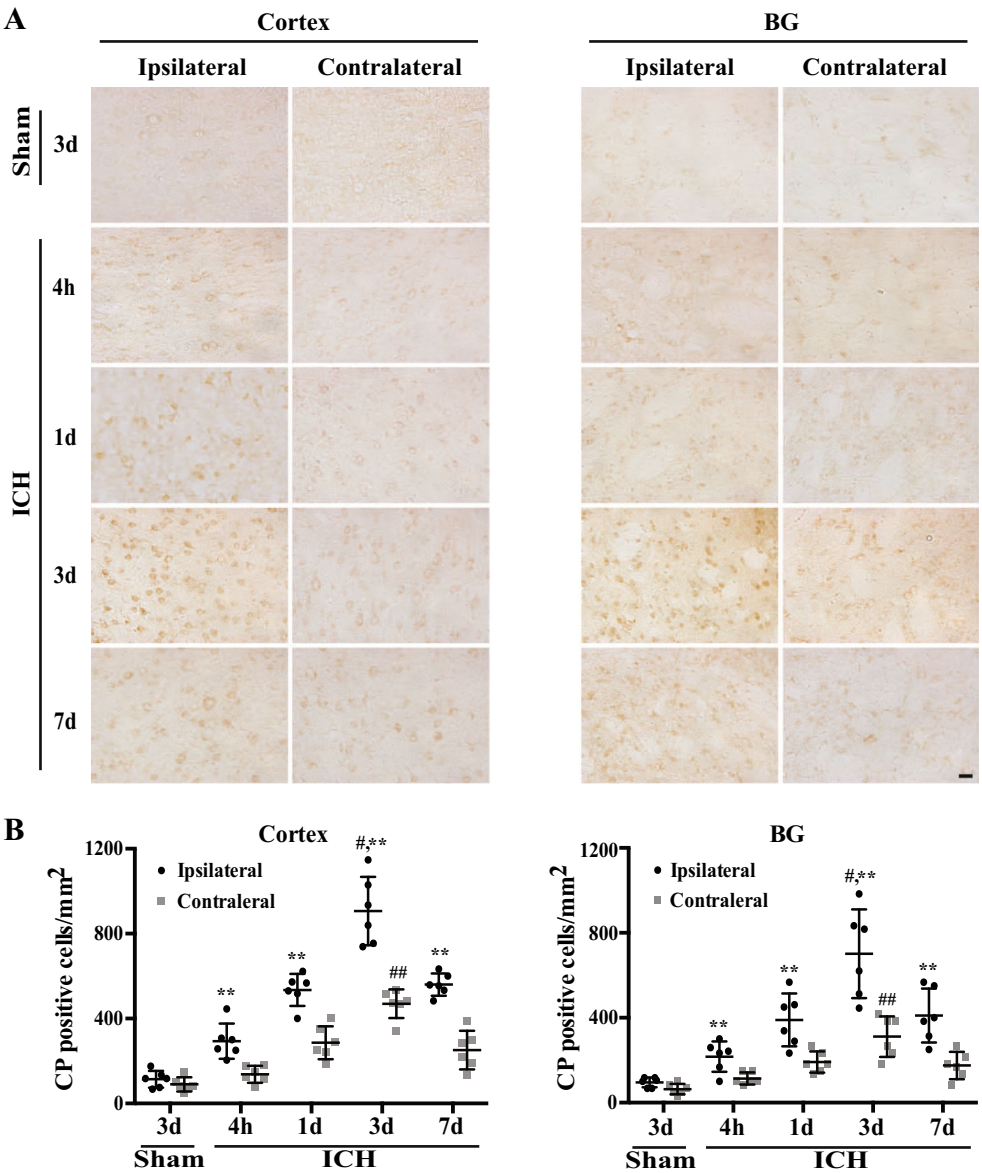

Fig. 1 Upregulation of ceruloplasmin (CP) in the brain after ICH. **a** CP immunoreactivity in the ipsi- and contralateral cortex and basal ganglia. Scale bar, 20 μm. **b** The number of CP-positive cells in the ipsi- and contralateral cortex and basal ganglia (BG) at different times after ICH and day 3 after sham operation. Values are means ± SD; $n = 6$, $^{\#}P < 0.01$ versus the other groups, $^{**}P < 0.01$ versus the contralateral side, $^{\#\#}P < 0.01$ versus the sham group

Results

There were few CP-positive cells in both ipsi- and contralateral cortex and basal ganglia at day 3 after sham operation. In contrast, CP-positive cells increased gradually in both ipsilateral cortex and basal ganglia at 4 h, peaked at day 3, and decreased at day 7 after ICH ($P < 0.01$; Fig. 1). There was also an increase in the number of CP-positive cells in the contralateral hemisphere at day 3 (Fig. 1b). However, the number of CP-positive cells in the ipsilateral hemisphere was significantly higher than in the contralateral hemisphere at each of the time points after ICH in both cortex and basal ganglia ($P < 0.01$; Fig. 1b).

To determine which cell types express CP, triple immunofluorescence staining was performed at day 3 after ICH. The results showed that CP immunoreactivity colocalized with NeuN (a neuronal marker, Fig. 2a) and GFAP (an astrocyte marker, Fig. 2b) in the perihematomal area after ICH. It did not colocalize with Iba-1 (a microglia/macrophage marker, Fig. 2c).

To test whether CP can be produced in the brain, CP mRNA was analyzed by RT-PCR. CP mRNA was detected in sham and ICH brains. Compared with the sham group, a significant increase CP mRNA expression in the basal ganglia was found in the day-3 ICH group (CP/GAPDH: 0.99 ± 0.03 versus 0.52 ± 0.08, $P < 0.01$; Fig. 2d).

T2 hyperintensity on MRI was used to indicate brain injury (T2 lesion) at 24 h after the injection of Fe^{2+} or Fe^{2+} + CP. Compared with saline injection, Fe^{2+} injection induced marked T2 lesion (36 ± 6 mm^3 versus 3 ± 1 mm^3 with saline; $P < 0.01$; Fig. 3a). Co-injection of CP with Fe^{2+} significantly reduced T2 lesion volume (14 ± 4 versus 36 ± 6 mm^3 with Fe^{2+} alone; $P < 0.01$; Fig. 3a).

To assess neurological deficits, corner-turn and forelimb-use asymmetry tests were used at day 1 after the injection of

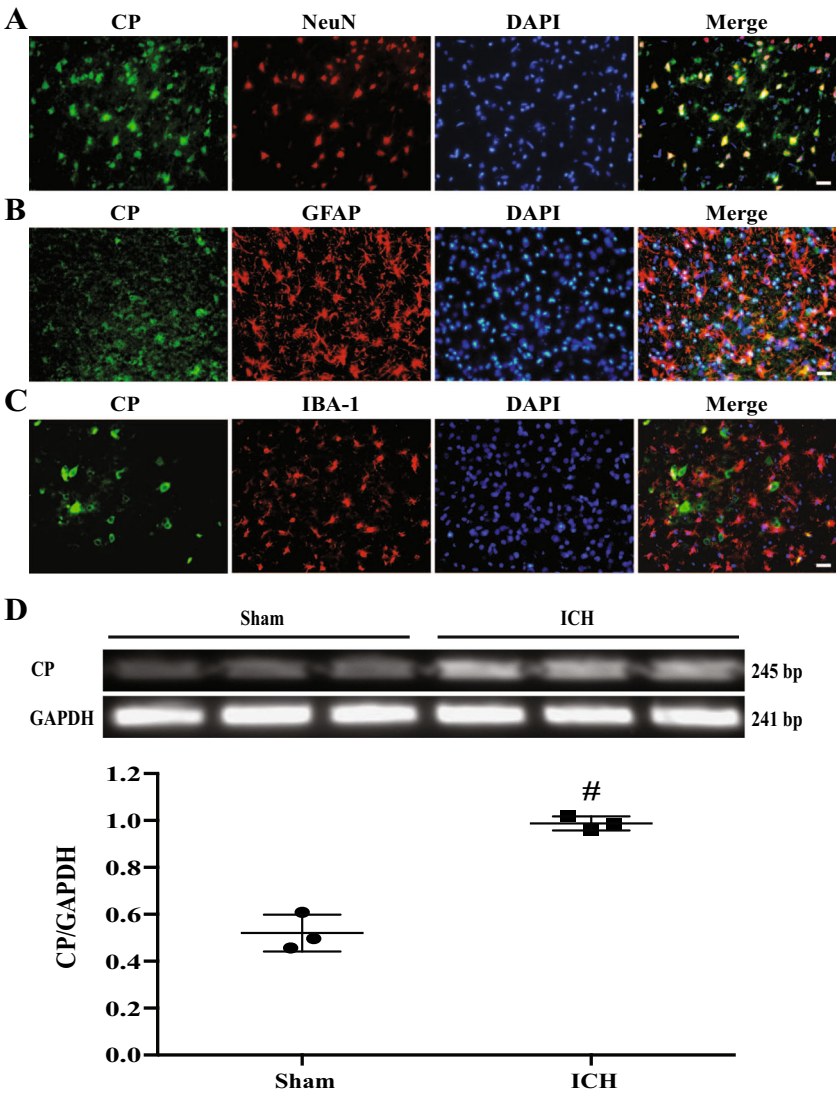

Fig. 2 Triple immunofluorescence labeling of CP, NeuN (**a**), GFAP (**b**), Iba-1 (**c**) in the perihematomal area at day-3 after ICH. Scale bar, 20 μm. Colocalization of CP with NeuN (neuronal) and GFAP (astrocytic) but not Iba-1 (microglial). **d** Expression of CP mRNA was determined by RT-PCR in the ipsilateral basal ganglia at day 3 after ICH and sham operation. Values (ratio to GAPDH) are means ± SD; $n = 3$, $^{\#}P < 0.01$

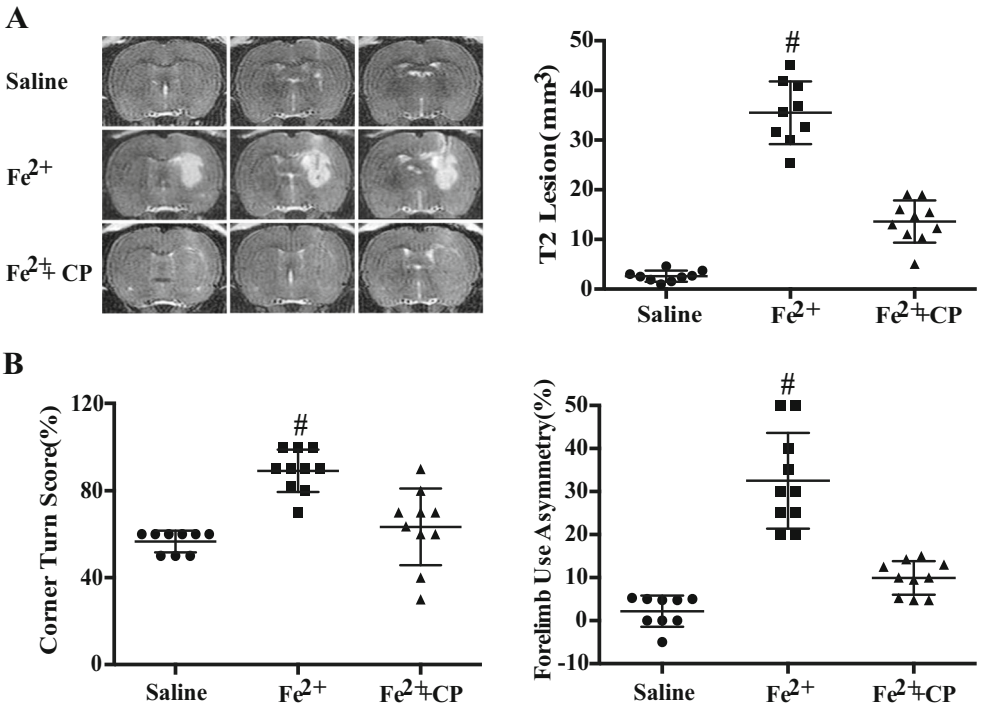

Fig. 3 Effects of intracerebral injection of ferrous iron with and without ceruloplasmin (CP) or saline on T2-weighted lesion size and behavioral deficits. **a** T2-weighted MRI lesions at day 1. Values are means ± SD; $n = 9–10$ per group, $^{\#}P < 0.01$ versus the other groups. **b** Corner-turn tests score and forelimb-use asymmetry at day 1. Values are means ± SD; $n = 9–10$ per group, $^{\#}P < 0.01$ versus the other groups

saline, Fe^{2+} or Fe^{2+} + CP. Compared with saline injection, ferrous iron injection induced significant neurological deficits (Fig. 3b). CP treatment significantly ameliorated neurological deficits induced by Fe^{2+} ($P < 0.01$; Fig. 3b).

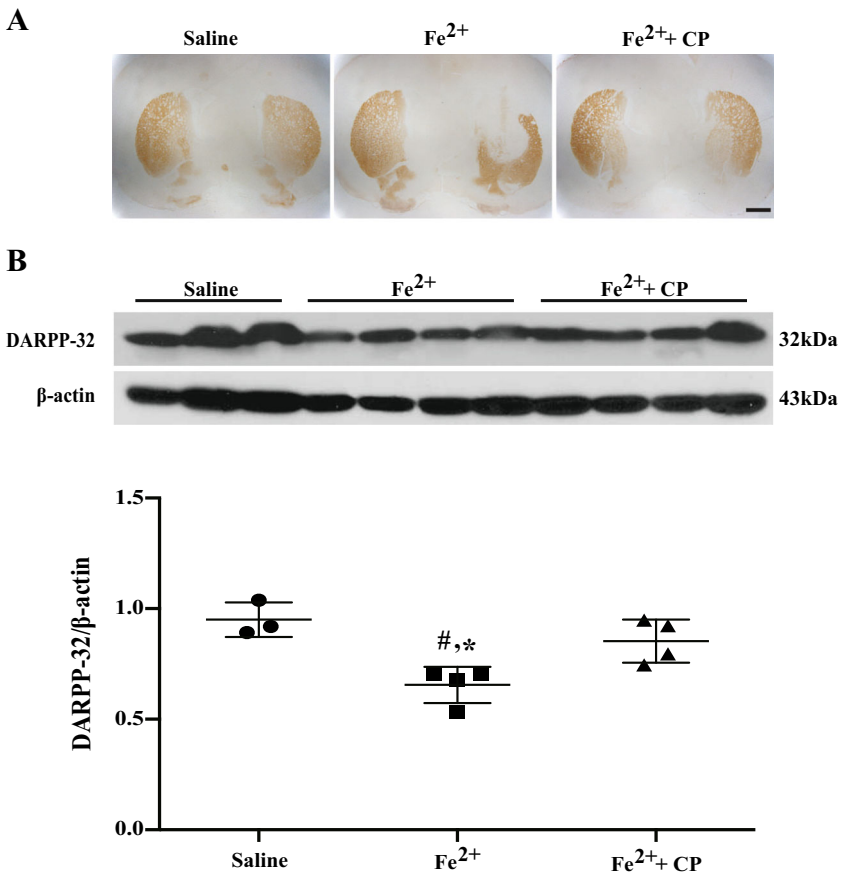

Fig. 4 Neuronal death in the basal ganglia at 24 h after intracerebral injection of ferrous iron with and without ceruloplasmin (CP) or saline. **a**) DARPP-32 immunoreactivity. Scale bar, 1 mm. **b** DARPP-32 protein levels determined by Western blot analysis in the ipsilateral basal ganglia. Values (ratio to β-actin) are means ± SD; $n = 3–4$ per group, $^{\#}P < 0.01$ versus saline group, $^{*}P < 0.05$ versus Fe^{2+} + CP group

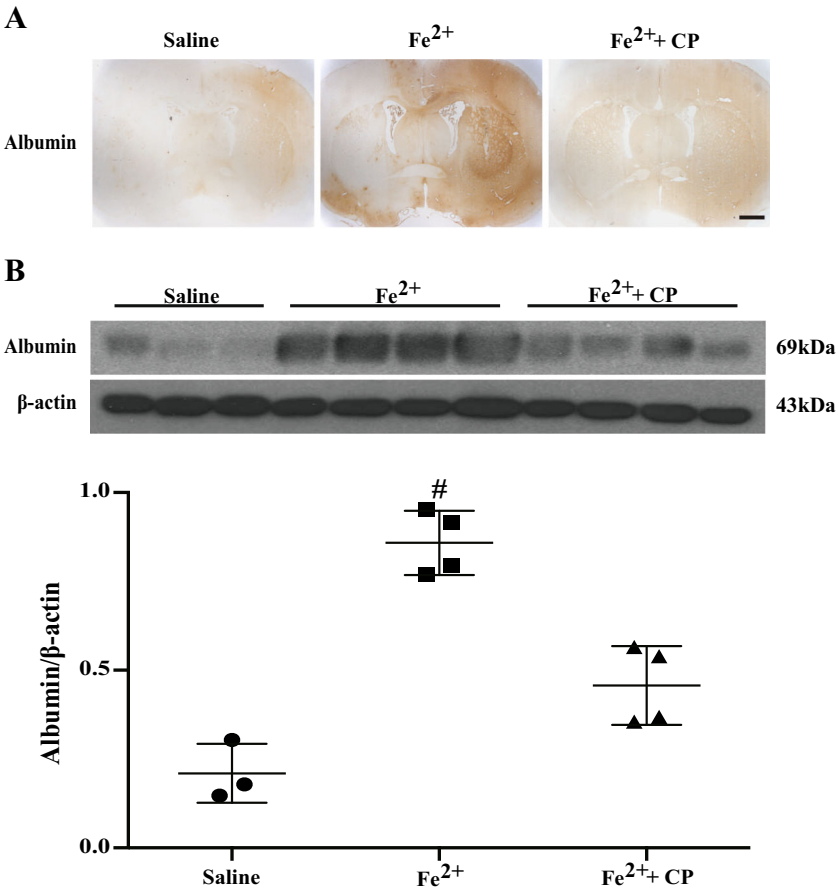

Fig. 5 Blood-brain barrier disruption after intracerebral injection of ferrous iron with and without ceruloplasmin (CP) or saline. **a** Albumin immunoreactivity at day 1 after injection. Scale bar, 1 mm. **b** Albumin protein levels, Western blot analysis, in the ipsilateral basal ganglia. Values (ratio to β-actin) are means ± SD; $n = 3$–4 per group, $^{\#}P < 0.01$ versus other groups

DARPP-32 is a specific and reliable marker for neuronal injury in the basal ganglia [9]. In this study, DARPP-32 levels in the ipsilateral basal ganglia were measured by immunochemistry staining and Western blot analysis at day 1 after iron injection. DARPP-32 protein levels in Fe^{2+} group were decreased significantly compared with saline group (DARPP/β-actin: 0.66 ± 0.08 versus 0.95 ± 0.08, $P < 0.01$; Fig. 4). CP treatment significantly reduced Fe^{2+}-induced basal ganglia neuronal death (DARPP-32/β-actin: 0.85 ± 0.09 versus 0.66 ± 0.08 $P < 0.05$; Fig. 4).

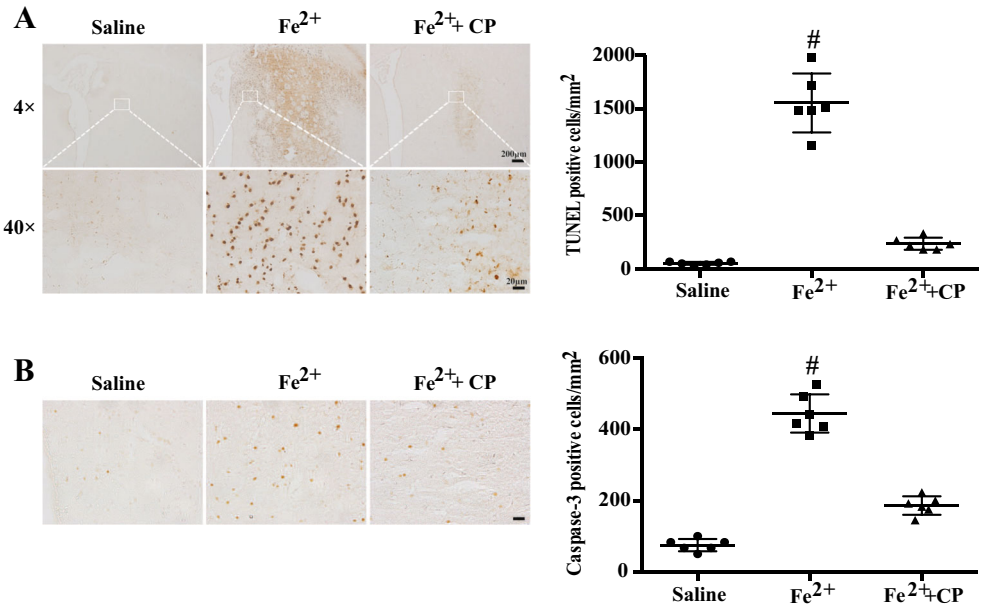

Fig. 6 Cell death after intracerebral injection of ferrous iron with and without ceruloplasmin (CP) or saline. **a** TUNEL-positive cells in ipsilateral basal ganglia of rats at day 1 after injection. Values are mean ± SD; $n = 6$, $^{\#}P < 0.01$ versus the other groups. Scale bars, 200 μm and 20 μm. **b** Cleaved caspase-3 immunoreactivity and number of positive cells in ipsilateral brain at day 1 after injection. Values are mean ± SD; $n = 6$, $^{\#}P < 0.01$ versus the other groups. Scale bar, 20 μm

Albumin was measured by immunohistochemistry and Western blots to assess the BBB disruption in the ipsilateral basal ganglia at day 1 after operation. Intracaudate Fe^{2+} injection caused marked BBB disruption (albumin/β-actin: 0.86 ± 0.09 versus 0.21 ± 0.08 in saline group; $P < 0.01$; Fig. 5). This was significantly reduced in the Fe^{2+} + CP group (albumin/β-actin: 0.46 ± 0.11 versus 0.86 ± 0.09 in Fe^{2+} group; $P < 0.01$; Fig. 5).

Brain cell death was examined by TUNEL staining at day 1 after intracerebral injection. Abundant TUNEL-positive cells were found in the ipsilateral basal ganglia after Fe^{2+} injection (Fig. 6a). CP treatment caused a significant reduction in TUNEL-positive cells around the injection area in the ipsilateral basal ganglia (238 ± 62/mm^2 versus 1558 ± 318/mm^2 in Fe^{2+} alone group; $P < 0.01$; Fig. 6a). The number of cleaved caspase 3-positive cells in Fe^{2+} + CP group was also much less than in the Fe^{2+} alone group (186 ± 37/mm^2 versus 445 ± 71/mm^2; $P < 0.01$; Fig. 6b).

Discussion

The major findings in the current study are as follows: (1) Brain CP levels are increased after ICH; (2) CP is expressed on neurons and astrocytes in cortex and basal ganglia after ICH; and (3) CP attenuates ferrous iron-induced brain injury and neurological deficits.

Ceruloplasmin is an important multi-copper oxidase with ferroxidase activity that oxidizes toxic Fe^{2+} to less-toxic Fe^{3+}, and promotes the combination of iron and transferrin, indirectly regulating the utilization and storage of iron [5, 15]. Brain iron accumulation caused by a lack of ceruloplasmin correlates with several neurodegenerative diseases, including Alzheimer's and Parkinson's disease [7, 16–18].

CP is an abundant plasma α2-glycoprotein, being mainly synthesized by hepatocytes and secreted into blood [19]. It cannot pass blood-brain barrier (BBB) in wild-type animals, although there is evidence that it can in CP knockout mice [15, 20, 21]. Previous studies have confirmed that the glycosylphosphatidylinositol (GPI)-anchored form of CP is expressed in the brain of human and rats, including in the cerebral cortex, basal ganglia, hippocampus, and cerebellum [6, 22]. The current study showed that CP mRNA as well as protein is expressed in the brain and upregulated after ICH. These results suggest that the nervous tissue can synthesize and secrete CP. Further studies are needed to determine how much brain CP after ICH is brain-derived rather than hematoma/blood-derived.

Thrombin and iron are two major players in ICH-induced brain injury, and both can upregulate brain CP levels. Thus, our previous experiments showed that thrombin upregulates brain CP mRNA and protein levels [23] and that intracerebral injection of iron also increases brain CP levels [24]. Iron, a hemoglobin degradation product, plays a crucial role in ICH-induced brain injury [2]. After ICH, erythrocyte lysis releases iron into the perihematomal zone. Iron overload can lead to brain edema, brain cell death, and neurological deficits after ICH [25–30]. Here, we found that Fe^{2+} causes marked brain cell death. Many dead cells had double-strand DNA damage (TUNEL-positive) and some were apoptotic (caspase-3 activation). It should be noted that serum CP concentrations are very high (300–450 μg/ml) [31]. We did not test whether or not exogenous CP can attenuate ICH-induced brain injury. In the current study, therefore, a Fe^{2+} injection rat model was used to examine whether exogenous CP can reduce Fe^{2+}-related brain injury. According to our previous study, Fe^{2+} (0.2 mM) with or without CP (10 μM) in 50 μl saline were used [23]. We found that CP can reduce Fe^{2+}-induced brain injury.

In this proof-of-concept study, we co-injected CP with Fe^{2+} to examine whether it would reduce brain injury by oxidizing toxic Fe^{2+} to the less toxic Fe^{3+}. Co-injection of CP significantly reduced BBB permeability, DNA damage, neuronal cell death, and neurological deficits at the first day. Future studies should examine whether CP can reduce acute and chronic brain injury after ICH. CP is the key regulator of iron homeostasis, and its deficiency has been shown to induce iron dysregulation in humans and animal models [7, 16, 21, 32]. There is some evidence indicating that CP loss increases neuronal susceptibility to ischemic injury and leads to neurodegeneration [15, 33]. CP is an important antioxidant that is effective in inhibiting lipid peroxidation and superoxide and inhibiting free-radical damage stimulated by iron [20, 31, 34].

In summary, the current study showed that CP expression is increased in neurons and astrocytes after ICH. This was associated with an increase in brain CP mRNA. Exogenous CP reduced ferrous iron-induced brain injury. These results suggest a role of CP in brain injury following ICH.

Funding This work was supported by grants NS-091545, NS-090925, NS-096917, and NS-106746 from the National Institutes of Health (NIH).

Compliance with Ethical Standards

Conflict of Interest The authors declare that they have no conflict of interest.

Ethical Approval All institutional and national guidelines for the care and use of laboratory animals were followed.

References

1. Xi G, Keep RF, Hoff JT. Mechanisms of brain injury after intracerebral hemorrhage. Lancet Neurol. 2006;5:53–63.

2. Wilkinson DA, Pandey AS, Thompson BG, Keep RF, Hua Y, Xi G. Injury mechanisms in acute intracerebral hemorrhage. Neuropharmacology. 2018;134:240–8.
3. Garton T, Keep RF, Wilkinson DA, Strahle JM, Hua Y, Garton HJ, et al. Intraventricular hemorrhage: the role of blood components in secondary injury and hydrocephalus. Transl Stroke Res. 2016;7: 447–51.
4. Xiong XY, Wang J, Qian ZM, Yang QW. Iron and intracerebral hemorrhage: from mechanism to translation. Transl Stroke Res. 2014;5:429–41.
5. Bielli P, Calabrese L. Structure to function relationships in ceruloplasmin: a 'moonlighting' protein. Cell Mol Life Sci. 2002;59: 1413–27.
6. Klomp LW, Farhangrazi ZS, Dugan LL, Gitlin JD. Ceruloplasmin gene expression in the murine central nervous system. J Clin Invest. 1996;98:207–15.
7. Texel SJ, Xu X, Harris ZL. Ceruloplasmin in neurodegenerative diseases. Biochem Soc Trans. 2008;36:1277–81.
8. Zheng M, Du H, Ni W, Koch LG, Britton SL, Keep RF, et al. Iron-induced necrotic brain cell death in rats with different aerobic capacity. Transl Stroke Res. 2015;6:215–23.
9. Jin H, Xi G, Keep RF, Wu J, Hua Y. Darpp-32 to quantify intracerebral hemorrhage-induced neuronal death in basal ganglia. Transl Stroke Res. 2013;4:130–4.
10. Dang G, Yang Y, Wu G, Hua Y, Keep RF, Xi G. Early erythrolysis in the hematoma after experimental intracerebral hemorrhage. Transl Stroke Res. 2017;8:174–82.
11. Hua Y, Xi G, Keep RF, Wu J, Jiang Y, Hoff JT. Plasminogen activator inhibitor-1 induction after experimental intracerebral hemorrhage. J Cereb Blood Flow Metab. 2002;22:55–61.
12. Ni W, Zheng M, Xi G, Keep RF, Hua Y. Role of lipocalin-2 in brain injury after intracerebral hemorrhage. J Cereb Blood Flow Metab. 2015;35:1454–61.
13. Wan S, Cheng Y, Jin H, Guo D, Hua Y, Keep RF, et al. Microglia activation and polarization after intracerebral hemorrhage in mice: the role of protease-activated receptor-1. Transl Stroke Res. 2016;7: 478–87.
14. Hua Y, Schallert T, Keep RF, Wu J, Hoff JT, Xi G. Behavioral tests after intracerebral hemorrhage in the rat. Stroke. 2002;33:2478–84.
15. Altamura C, Squitti R, Pasqualetti P, Gaudino C, Palazzo P, Tibuzzi F, et al. Ceruloplasmin/transferrin system is related to clinical status in acute stroke. Stroke. 2009;40:1282–8.
16. Kristinsson J, Snaedal J, Torsdottir G, Johannesson T. Ceruloplasmin and iron in Alzheimer's disease and Parkinson's disease: a synopsis of recent studies. Neuropsychiatr Dis Treat. 2012;8:515–21.
17. Vassiliev V, Harris ZL, Zatta P. Ceruloplasmin in neurodegenerative diseases. Brain Res Rev. 2005;49:633–40.
18. Kaneko K, Hineno A, Yoshida K, Ikeda S. Increased vulnerability to rotenone-induced neurotoxicity in ceruloplasmin-deficient mice. Neurosci Lett. 2008;446:56–8.
19. Chang YZ, Qian ZM, Du JR, Zhu L, Xu Y, Li LZ, et al. Ceruloplasmin expression and its role in iron transport in c6 cells. Neurochem Int. 2007;50:726–33.
20. Patel BN, Dunn RJ, Jeong SY, Zhu Q, Julien JP, David S. Ceruloplasmin regulates iron levels in the cns and prevents free radical injury. J Neurosci. 2002;22:6578–86.
21. Zanardi A, Conti A, Cremonesi M, D'Adamo P, Gilberti E, Apostoli P, et al. Ceruloplasmin replacement therapy ameliorates neurological symptoms in a preclinical model of aceruloplasminemia. EMBO Mol Med. 2018;10:91–106.
22. Patel BN, Dunn RJ, David S. Alternative rna splicing generates a glycosylphosphatidylinositol-anchored form of ceruloplasmin in mammalian brain. J Biol Chem. 2000;275:4305–10.
23. Yang S, Hua Y, Nakamura T, Keep RF, Xi G. Upregulation of brain ceruloplasmin in thrombin preconditioning. Acta Neurochir Suppl. 2006;96:203–6.
24. Zhao F, Xi G, Liu W, Keep RF, Hua Y. Minocycline attenuates iron-induced brain injury. Acta Neurochir Suppl. 2016;121:361–5.
25. Gaasch JA, Lockman PR, Geldenhuys WJ, Allen DD, Van der Schyf CJ. Brain iron toxicity: differential responses of astrocytes, neurons, and endothelial cells. Neurochem Res. 2007;32:1196–208.
26. Welch KD, Davis TZ, Van Eden ME, Aust SD. Deleterious iron-mediated oxidation of biomolecules. Free Radic Biol Med. 2002;32:577–83.
27. Calabrese V, Lodi R, Tonon C, D'Agata V, Sapienza M, Scapagnini G, et al. Oxidative stress, mitochondrial dysfunction and cellular stress response in friedreich's ataxia. J Neurol Sci. 2005;233:145–62.
28. Shamoto-Nagai M, Maruyama W, Yi H, Akao Y, Tribl F, Gerlach M, et al. Neuromelanin induces oxidative stress in mitochondria through release of iron: mechanism behind the inhibition of 26s proteasome. J Neural Transm. 2006;113:633–44.
29. Garton T, Keep RF, Hua Y, Xi G. Brain iron overload following intracranial haemorrhage. Stroke Vasc Neurol. 2016;1:172–84.
30. Karwacki Z, Kowianski P, Dziewatkowski J, Domaradzka-Pytel B, Ludkiewcz B, Wojcik S, et al. Apoptosis in the course of experimental intracerebral haemorrhage in the rat. Folia Morphol (Warsz). 2005;64:248–52.
31. David S, Patel BN. Ceruloplasmin: structure and function of an essential ferroxidase. Adv Struct Biol. 2000;6:211–37.
32. Zhao L, Hadziahmetovic M, Wang C, Xu X, Song Y, Jinnah HA, et al. Cp/heph mutant mice have iron-induced neurodegeneration diminished by deferiprone. J Neurochem. 2015;135:958–74.
33. Texel SJ, Zhang J, Camandola S, Unger EL, Taub DD, Koehler RC, et al. Ceruloplasmin deficiency reduces levels of iron and bdnf in the cortex and striatum of young mice and increases their vulnerability to stroke. PLoS One. 2011;6:e25077.
34. Shin EJ, Jeong JH, Chung CK, Kim DJ, Wie MB, Park ES, et al. Ceruloplasmin is an endogenous protectant against kainate neurotoxicity. Free Radic Biol Med. 2015;84:355–72.